Magnetic Island Formation by External Cyclic Perturbation in Rotating and Non-rotating Plasmas

Yasutomo ISHII

Japan Atomic Energy Agency, Ibaraki 311-0193, Japan

(Received 21 July 2009 / Accepted 8 October 2009)

Effects of a non-monotonically evolving external perturbation on a plasma, that is stable against tearing modes, are numerically investigated. It is found that for a magnetic island driven by an external single-cycle magnetic perturbation, the time constants during the phases of growth and decay are different. This difference in time constants causes a finite magnetic island to form even after the external perturbation is removed. Therefore, the saturation width of a magnetic island driven by a successive applications of an external single-cycle perturbation becomes larger than the maximum magnetic island width driven by a single application of that. For a rotating plasma, the background rotation is damped as the magnetic island grows due to an external perturbation [R. Fitzpatrick, Phys. Plasmas **5**, 3325(1998)]. Therefore, for a rotating plasma, the driven magnetic island can enter an explosive growth stage due to successive applications of a single-cycle perturbation even with amplitude smaller than the critical value for the onset of the rapid growth in the case of a monotonically increasing or step-function type external perturbation. These features are important in explaining the explosive growth of magnetic islands and the onset of neoclassical tearing mode due to non-monotonically growing MHD phenomena such as sawtooth, fishbones and ELM.

Keywords: magnetic island, plasma rotation, external perturbation, neoclassical tearing mode, sawtooth

DOI: 10.1585/pfr.5.002

1. Introduction

In tokamak plasma, some magnetohydrodynamics (MHD) activities such as a neoclassical tearing mode (NTM) [1], a resistive wall mode (RWM) [2], etc. can be triggered by external perturbations. Also, the resonant magnetic perturbation (RMP) [3], which is an externally applied magnetic perturbation with helicity resonant to the rational surface in the plasma edge region, is considered an effective way to control the edge localized mode (ELM) [4]. For the onset condition and the control of MHD phenomena by external perturbation, it has been pointed out that the interaction between the external perturbation and the plasma rotation is important. Magnetic island formation due to external perturbations is important from the viewpoint of seed magnetic island formation for NTM. Also, plasma rotation damping by external perturbations is considered to be a fundamental process of RWM onset in rotating plasmas. In previous studies [5–7], to estimate the onset condition of the rapid magnetic island growth in rotating plasmas, externally applied perturbations were modeled by a static (step-function type) magnetic perturbation and a perturbation increasing monotonically in time. These models of external perturbations might be suitable for RMP and the error magnetic field. However, ELM and other MHD modes, such as the sawtooth [8], destabilized at a radial position different from the resonance surface of the target mode may act as an external perturbation for the target mode, through the toroidal or nonlinear mode coupling. Usually, MHD modes non-monotonically grow, saturate, and/or decrease until gone. For sawtooth and ELM, these modes appear periodically. To model such MHD modes, one should not to use a static or monotonically increasing external perturbation, but instead use a non-monotonically increasing and periodic perturbation. In the current study, the effects of external periodic perturbations on rotating or non-rotating plasmas, that are stable for the tearing mode, are investigated to understand the formation process of a magnetic island driven by non-monotonically growing MHD phenomena such as sawtooth, ELM, fishbone, etc.

2. Numerical Model

In the current study, we investigate the effects of non-monotonically increasing external perturbations on magnetic island formation at a tearing stable resonant surface. We consider the helical mode with $m/n = 2/1$, where m and n are the poloidal and toroidal mode numbers, in a cylindrical plasma with a safety factor profile (q-profile), and a plasma rotation profile, as shown in Fig. 1. The safety factor profile is $q = q_0 \cdot \{1 + (r/r_0)^2\}$ with $q_0 = 0.7$ and $r_0 = 0.603$. This q profile has the resonance surface of the $m/n = 2/1$ mode at $r = 0.82$ and is stable against the tearing mode ($\Delta' < 0$). For this study, the plasma rotation

author's e-mail: ishii.yasutomo@jaea.go.jp

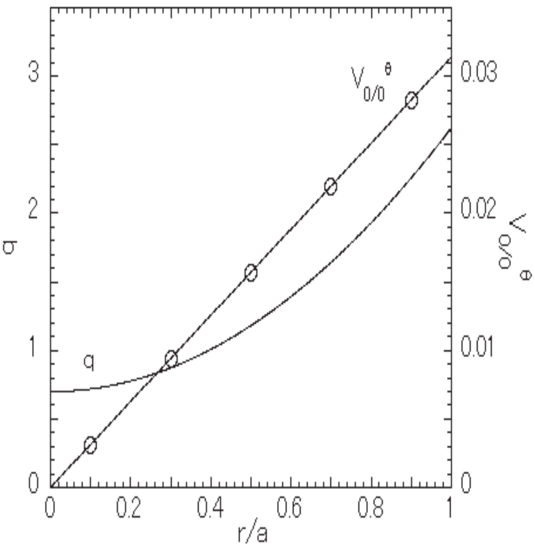

Fig. 1 Safety factor (q-profile, solid line) and the poloidal background rotation $V^{\theta}_{0/0}$ profile (marked line) used in this study.

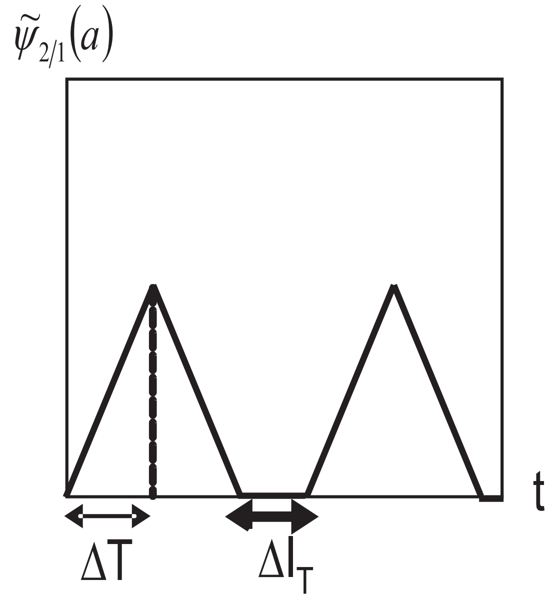

Fig. 2 Schematic of the time evolution of an external magnetic perturbation at the plasma surface $r = a$, $\tilde{\psi}_{2/1}(a)$. ΔT is the time interval during which $\tilde{\psi}_{2/1}(a)$ increases and decreases. ΔI_{T} is the time interval during which $\tilde{\psi}_{2/1}(a) = 0$.

is initially set as $V_\theta = \Omega r$, where the angular velocity Ω is constant indicating the rigid plasma rotation.

For this plasma, we impose a magnetic flux perturbation at the plasma edge, $\tilde{\psi}_{2/1}(a)$. Figure 2 shows the waveform of $\tilde{\psi}_{2/1}(a)$. The time labeled ΔT is increasing/decreasing time of the phase, and the time labeled ΔI_{T} is the time during which the perturbation is zero at the plasma edge. For a single-cycle of duration $2\Delta T$, the magnetic flux perturbation at the plasma edge, $\tilde{\psi}_{2/1}(a)$ is

$$\tilde{\psi}_{2/1}(t,a) = \begin{cases} A \cdot \psi^{\theta}_{0/0}(t=0,a) \cdot t & \text{for } t \leq \Delta T \\ A \cdot \psi^{\theta}_{0/0}(t=0,a) \cdot (t_0 - t) & \text{for } \Delta T \leq t \leq 2 \cdot \Delta T. \end{cases} \tag{1}$$

Here, $\psi^{\theta}_{0/0}(t = 0, a)$ is the equilibrium poloidal flux at $r = a$ and $t = 0$, and A is a coefficient. For this study, we use $A = 10^{-5}$. The quantity $\psi^{\theta}_{0/0}$ is normalized as $\psi^{\theta}_{0/0}(a) = aB_0\bar{\psi}^{\theta}_{0/0}(a)$.

To study the nonlinear evolution of the MHD mode for this externally applied magnetic perturbation, we employ a reduced set of MHD equations [9] with helical symmetry. We solve these equations using the predictor collector time integrating method with the finite difference expression for the radial coordinate and the Fourier mode expansion for the Azimuthal coordinate. This treatment yields

$$\frac{\partial}{\partial t}\psi = \frac{1}{r}[\psi, \phi] + \frac{B_0}{R_0}\frac{\partial}{\partial \varphi}\phi + \eta J \tag{2}$$

$$\frac{\partial}{\partial t}U = \frac{1}{r}[U, \phi] + \frac{1}{r}[\psi, J] + \frac{B_0}{R_0}\frac{\partial J}{\partial \varphi} + \mu \nabla^2_{\perp} U \tag{3}$$

$$J = \nabla^2_{\perp}\psi, \ U = \nabla^2_{\perp}\phi$$

$$[\mathrm{a,b}] = \frac{\partial a}{\partial r}\frac{\partial b}{\partial \theta} - \frac{\partial b}{\partial r}\frac{\partial a}{\partial \theta}$$

where, ψ is the poloidal flux function, ϕ is the flow potential, J is the plasma current, U is the vorticity, φ is the toroidal angle, B_0 is the toroidal magnetic field at the magnetic axis, R_0 is the aspect ratio, which is set to 10 in this study. These equations include the resistivity η and the viscosity μ. For the initial background component of the vorticity, we use $U_0 = 2\Omega$. In Eqs. (2) and (3), the parameters are normalized by the plasma minor radius a and the poloidal Alfven time $\tau_{\mathrm{pa}} = \sqrt{\rho}a/B_\theta(a)$, where the plasma density ρ is set to 1. The resistivity η is normalized such that $\eta = \tau_{\mathrm{pa}}/\tau_\eta$, where $\tau_\eta = a^2/\eta$ is the plasma skin time. The viscosity ν is normalized such that $\nu = \tau_{\mathrm{pa}}/\tau_\nu$, where $\tau_\nu = a^2/\nu$ is the visco diffusion time. In this study, $\eta = 10^{-5}$ and $\nu = 10^{-7}$ are used for nonlinear calculations.

We now discuss the boundary conditions used in this study. The plasma is no longer an isolated system, because the magnetic energy is exchanged by varying $\psi_{2/1}$ at the plasma boundary. Except for plasma boundary $r = 1$, the ψ and U (i.e. ϕ) obey MHD equations (2) and (3). For the fixed boundary condition, $\tilde{\phi} = 0$ at the boundary $r = 1$, which is inconsistent with the inner plasma. To avoid this inconsistency, the boundary condition for $\phi_{2/1}$ is,

$$\phi_{2/1}(a) = \frac{q(a)}{2 - q(a)}\frac{\partial}{\partial t}\psi_{2/1}(a). \tag{4}$$

Here, the resistivity effect, which becomes important at the resonant surface, is neglected. The finite ψ at the boundary yields the Reynolds Stress. The Reynolds effect here is of 2nd order in the perturbation. Therefore, to consider a large external perturbation, we must consider a more appropriate boundary condition.

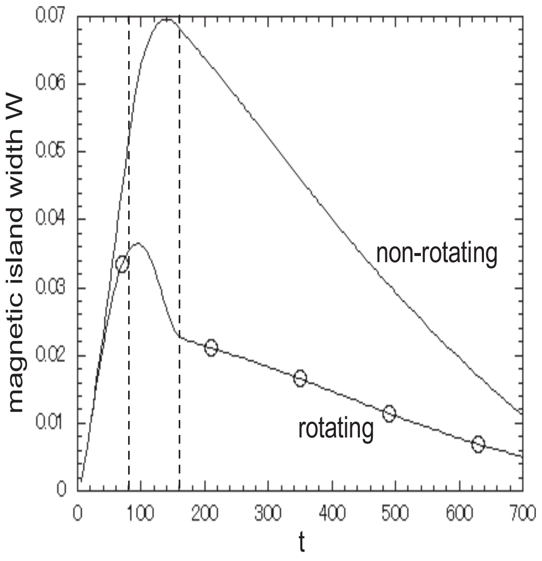

Fig. 3 Evolution of an externally driven magnetic island in non-rotating (solid line) and rotating (marked line) plasmas driven by an external single-cycle perturbation. $\Delta T = 80$.

3. Application of an External Single-cycle Perturbation

We consider first the application of single-cycle perturbation at the plasma edge, that corresponds to infinity of ΔI_T, in order to investigate the basic process of an externally driven magnetic island evolution. Figure 3 shows the evolution of the magnetic island width in a non-rotating plasma (solid line) and a rotating one (marked line) both driven by a single-cycle external perturbation with $\Delta T = 80$ and with a maximum value of $\tilde{\psi}_{2/1}(a) = 8.0 \times 10^{-4} \times \psi_{0/0}(0, a) = 7.2 \times 10^{-4}$, where $\psi_{0/0}(0, a)$ is the initial equilibrium poloidal flux function at the plasma edge. For example, the critical amplitude, estimated using a monotonically increasing external perturbation, is $\tilde{\psi}_{2/1}(a) = 1.25 \times 10^{-3}$ for the parameters used in this study. Figure 4 shows the evolution of the magnetic perturbation profiles in both plasmas. For single-cycle perturbation, the evolution of the magnetic island width is divided into two stages for a non-rotating plasma and three stages for a rotating plasma. The scalings for the time constant for the plasma resistivity in each stage are plotted in Fig. 5.

In the first stage, the magnetic island grows with the external perturbation and the time constant of this initial growth phase is almost the same for both rotating and non-rotating plasmas. This process is the conventional forced magnetic reconnection and the time scale is proportional to $\eta^{1/3}$, as shown in Fig. 5. For non-rotating plasmas, even after the external perturbation begins to decrease, the driven magnetic island continues to grow. As shown in Fig. 4, the magnetic perturbation in the region outside the resonant surface still has a large gradient toward the resonant surface. Therefore, the magnetic perturbation is pushed toward the resonant surface and the magnetic field is forced-reconnected. This process delays the timing for the magnetic island width to start to decrease by $\Delta t \approx 60$, which is a large fraction of $\Delta T = 80$. After the magnetic perturbation gradient reverses (Figs. 4 (g) and (h)), the magnetic perturbation inside the resonance surface starts to decrease due to the dissipation at the resonance surface. This is the resistive diffusion process and the scaling of the time constant is proportional to the plasma resistivity, as shown in Fig. 5 (a).

For a rotating plasma, a part of the magnetic perturbation energy injected from the plasma edge is used to decelerate the plasma rotation near the resonance surface and the perturbation just outside the resonance surface is maintained at a level lower than that maintained for a non-rotating plasma, as shown in Fig. 4 (d). The width of the magnetic island starts to decay shortly after the external perturbation begins to decrease. In this case, the time elapsed until the width of the magnetic island begins to decay also increases by $\Delta t \approx 20$. Although this value is small compared to the corresponding value for a non-rotating plasma, it still plays an important role in the evolution of the island. It is also interesting to note that the scaling of the time constant in this stage of the decay is similar to that of the forced reconnection in the growing stage, as shown in Fig. 5 (b). Although the physics of this scaling is not clearly understood at present, the perturbed current profile, i.e. the perturbed magnetic flux profile, near the $q = 2$ resonant surface in the rotating plasma is modified compared to that in the non-rotating plasma. The reason for this is the Alfven resonance shift by a plasma rotation, as shown in the previous studies [10–12]. This Alfven resonance effect causes an outward shift of the minimum point of the magnetic perturbation from the $q = 2$ resonant surface. Therefore, a large local gradient of the magnetic field forms near the resonance surface and this may cause the dissipation of the magnetic flux under the compressed state of the magnetic field, like the forced reconnection for the increasing phase. When this local gradient becomes small, the evolution of the magnetic island enters the third stage, where the magnetic perturbation decays through resistive diffusion as shown in Fig. 5 (b).

The important point of these simulation results is that the magnetic island survives with a finite width for a long time after the single-cycle of the external perturbation. As noted before, this is caused by the combined effects of the time lag between the evolutions of the magnetic island width and the external magnetic perturbation, and the slower decay rate of resistive diffusion after the external perturbation ceases.

4. Application of an External Multiple-pulse Perturbation in a Non-rotating Plasma

The discrepancy between the evolution of a magnetic

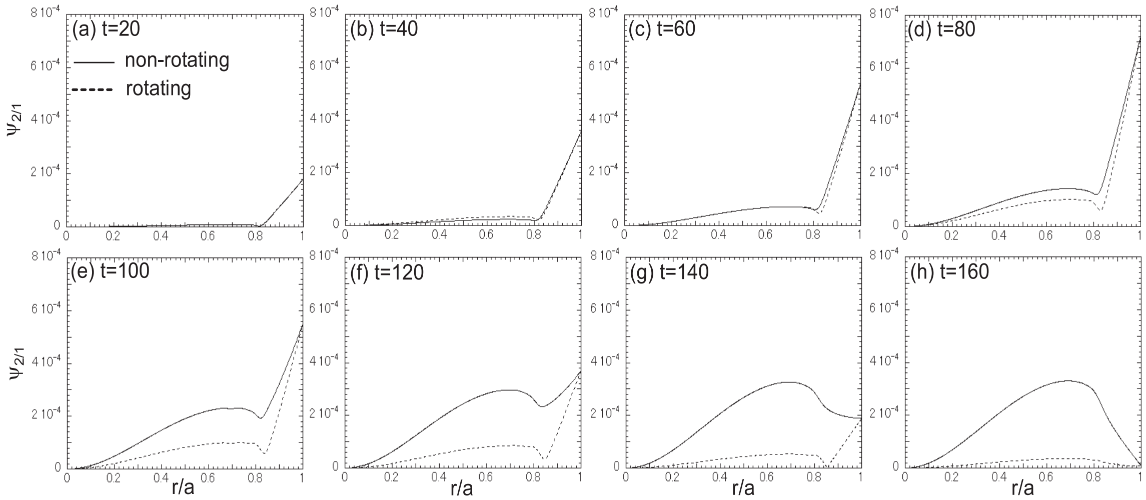

Fig. 4 Time evolution of the radial profile of the magnetic flux $\psi_{2/1}$. Absolute value of $\psi_{2/1}$, $|\psi_{2/1}| = \sqrt{(\psi^r_{2/1})^2 + (\psi^i_{2/1})^2}$, is plotted. $\psi^r_{2/1}$ is the real part of $\psi_{2/1}$ and $\psi^i_{2/1}$ is the imaginary part of that.

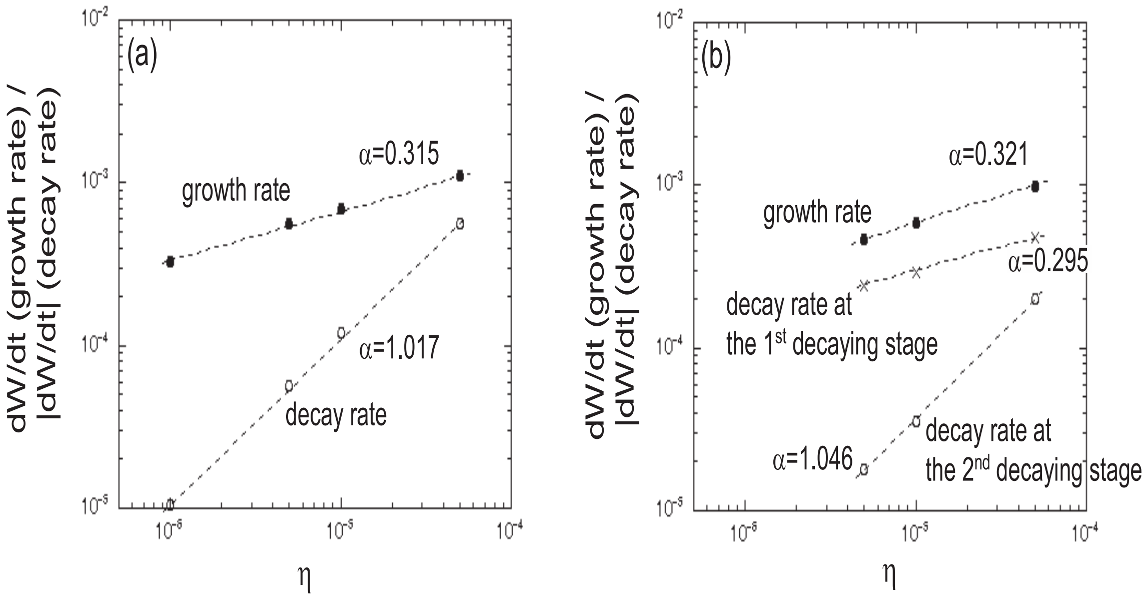

Fig. 5 Scaling of an externally driven magnetic island width with the resistivity for (a) non-rotating and (b) rotating plasmas. This scaling is estimated by assuming $\frac{dW}{dt} \propto \eta^\alpha$. The solid circles indicate the stage during which the island is increasing in size and the open circles are for the stage where the island is decreasing in size.

island and the external perturbation and the nonsymmetric growing and decaying time scale (see Figures 3 and 5) imply that the magnetic island does not vanish at the end of a single external perturbation cycle ($t = 2\Delta T$) at the plasma edge. Therefore, the repetition of an external perturbation could result in the cumulation of the magnetic perturbation in the plasma. Figure 6 shows the time evolution of the magnetic island width driven by successive applications of a an external cyclic external perturbation with different a time interval, ΔI_T, in the no-rotating plasma. For a reference, the magnetic island width evolution for a step-function type external perturbation is also plotted. For a step-function type external perturbation, $\tilde{\psi}_{2/1}(a)$ increases during $\Delta T = 80$ and remains constant without a decreasing phase after $t = 80$. For $\Delta I_T = 0$, the island width increases with oscillations. After about 10 cycles, it saturates at $W_{max} \approx 0.097$ with small amplitude oscillations. The saturation width of the magnetic island is smaller than that for an external step-function type perturbation. The reduction of the saturation amplitude is about $1/\sqrt{2}$, which is the square root of the average amplitude of the external oscillating perturbation. Increasing the time interval ΔI_T between perturbations weakens the cumulation effect and the saturated magnetic island width becomes smaller. For

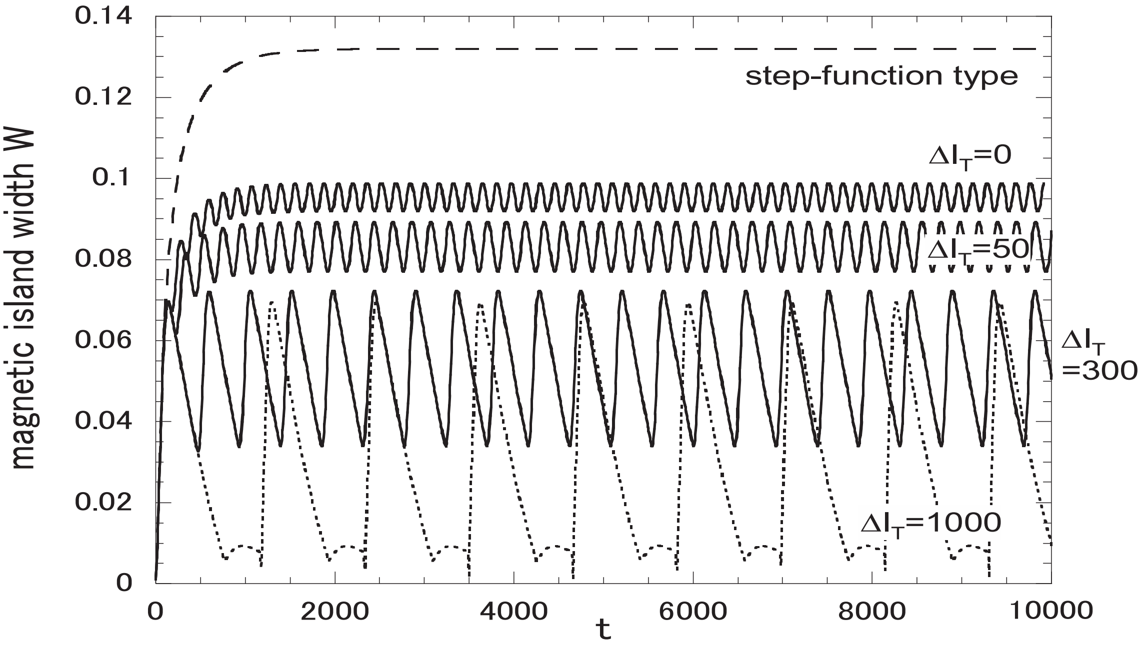

Fig. 6 Evolution of magnetic islands driven by external cyclic perturbations with different ΔI_T in a non-rotating plasma. Evolution of a magnetic island driven by an external step-function type perturbation is also shown as a reference.

$\Delta I_T = 1000$, W_{max} is about 0.069, which is almost the same value as that obtained for an external single-cycle one cycle perturbation.

5. Application of an External Multiple Multi-pulse Perturbation in a Rotating Plasma

Finally, we discuss the effects of successive applications of an external cyclic magnetic perturbation on a driven magnetic island formation in rotating plasma. For a step-function type or an external monotonically-increasing perturbation, previous research [5–7] has shown that the magnetic island enters a rapid growth stage in rotating plasmas, when the amplitude of the external perturbation exceeds a critical value. As shown in Fig. 3, for an external non-monotonic perturbation, when the amplitude of the external perturbation is below the critical value, the magnetic island decays as the external perturbation decreases and W_{max} for rotating plasmas is smaller than that for non-rotating plasmas.

Figure 7 show the time evolution of a magnetic island driven by successive applications of an external cyclic perturbation with different ΔI_T and the corresponding evolution of the plasma rotation velocity, $V^{\theta}_{0/0}$, at the resonance surface. For $\Delta I_T = 1000$, during $0 \leq t \leq 20000$, the magnetic island width is smaller than that in a non-rotating plasma. However, the plasma flow at the resonance surface gets decelerated every time an external perturbation cycle is applied, and the magnetic island grows gradually to saturate at the same width as found for the non-rotating plasma (Fig. 7 (a)). Note that the plasma flow at the resonance surface increases during the time interval ΔI_T in which there is no external magnetic perturbation. Thus, it takes a long time for the plasma flow to decrease to zero. The important aspect of this result is that, although successive applications of an external cyclic perturbation decreases the plasma flow, it does not cause the rapid growth of the magnetic island in this case, because the saturation width is not large enough for rapid growth.

For $\Delta I_T = 0$ and $\Delta I_T = 50$, after the rapid decay of the flow velocity and the growth of the magnetic island, the magnetic island enters the first saturation stage with almost the same saturation width for $\Delta I_T = 1000$. Corresponding to this first saturation of the magnetic island width, the flow velocity also enters the saturation state, oscillating at the same frequency as the external perturbation. During this first saturation stage, the magnetic island width deceases gradually. We note that, in contrast to the case of a monotonically increasing external perturbation, the temporal accumulation effect also affects the flow velocity at the resonance surface for the case of application of an external cyclic perturbation. Furthermore, the flow velocity also decreases in the same manner as for the monotonically increasing external perturbation. When the flow velocity decreases to zero level, the magnetic island grows explosively.

The physics of this explosive growth of the magnetic island in the rotating plasma is same as for a monotonically increasing external perturbation [5–7]. However, these results show that, even for a perturbation with amplitude below the critical value for the step function type or mono-

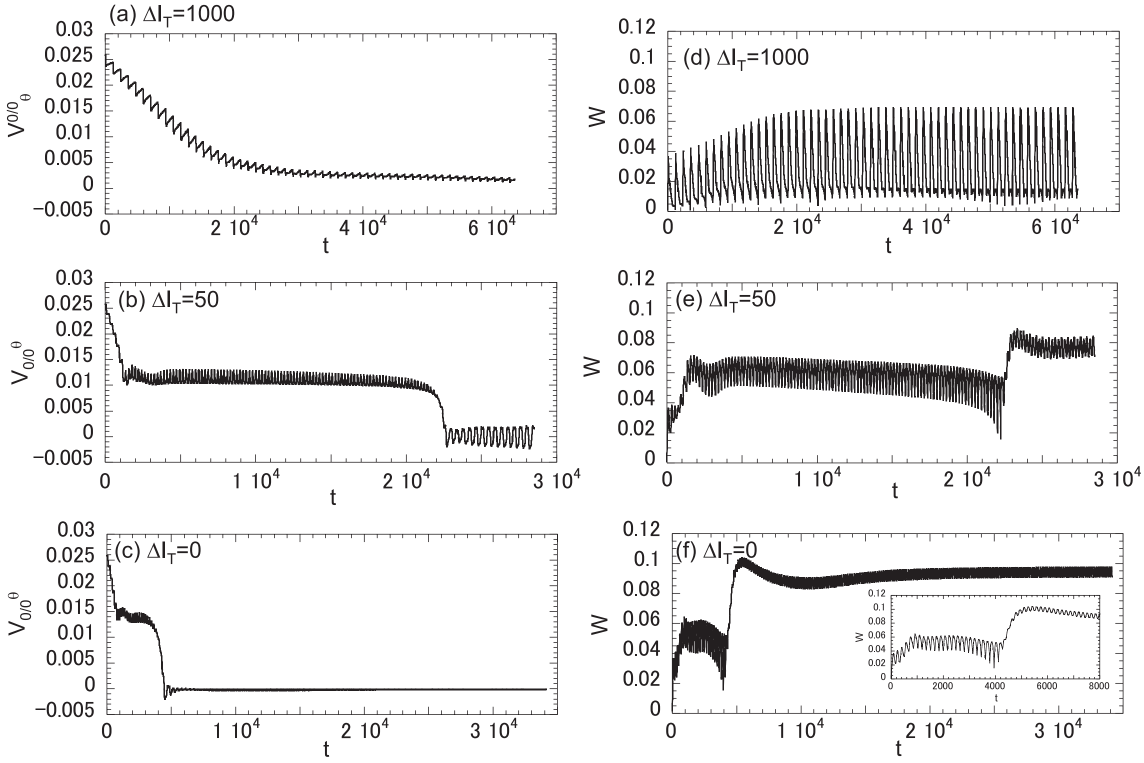

Fig. 7 Evolution of the flow velocity at the resonance surface and magnetic island width driven by external cyclic perturbations with different ΔI_T in rotating plasma. For (a) and (d) $\Delta I_T = 1000$, (b) and (e) $\Delta I_T = 50$, and for (c) and (f) $\Delta I_T = 0$. In (f), the inset shows a detailed view of the evolution of the magnetic island.

tonically increasing perturbation, successive applications of an external cyclic perturbation can effectively decrease the flow velocity at the resonance surface and induces the explosive growth of the magnetic island.

6. Summary and Discussion

In this study, effects of an external magnetic perturbation that evolves non-monotonically in time on a plasma that is stable against tearing modes are investigated. For single application of a monotonically increasing external perturbation, it is found that the time constants of the evolution of a magnetic island during the stage in which the external perturbation grows is different from the time constant during the stage in which the external perturbation decays. Furthermore, the two time constants scale differently with the plasma resistivity. This nonsymmetry in the time constants, and the different dynamics of the the magnetic island and the external perturbation result in the formation of a residual island after the external perturbation ceases. Because the time constant of the decaying phase is proportional to the resistivity and is much longer than that of the growing phase, this residual effect is more profound in higher temperature plasmas. As a result, in both non-rotating and rotating plasmas, the saturation width of a magnetic island for successive applications of an external cyclic perturbation is larger than the maximum magnetic island width for an external single-cycle perturbation. In rotating plasmas, we also find that, during the first saturation stage, the rotation velocity at the resonance surface continues to decrease even for successive applications of a sub-critical external perturbation. When the rotation velocity is small or zero, the magnetic island grows explosively to almost the same saturation width as that for the non-rotating plasma. This process is similar to that due to the application of an external step-function type or monotonically increasing perturbation. In this study, we have shown that, even for an external perturbation with amplitude smaller than the critical value, the magnetic island can enter the explosive growth stage by successive applications of such a sub-critical external cyclic magnetic perturbation.

The excitation of a magnetic island by an external perturbation is important as a basic process for the formation of a seed magnetic island for NTM. A seed magnetic island width larger than the threshold value can destabilize NTM . Therefore, if an externally driven magnetic island width becomes larger than this threshold value, this magnetic island can destabilize NTM. In previous studies on the evolution of a driven magnetic islands in rotating plasmas, monotonically increasing or step type external perturbations were considered to model an external magnetic perturbation. Therefore, the onset condition for a driven magnetic island is estimated from the amplitude of the external perturbation. This external perturbation model and the critical condition for the rapid magnetic island growth are considered to be suitable for the formation of a seed magnetic island by an error field, RMP, and non-periodic MHD phenomenon. However, in tokamak plasmas, sawtooth [13–16], fishbones [17, 18] and ELM [19, 20] are periodic phenomena and are seen as source MHD activities to excite a seed magnetic island. In those cases, NTM is not always observed during the first pulse, but rather after several pulses of a periodic MHD phenomenon [15]. Moreover, the onset timing of NTM does not always coincide with the maximum amplitude pulse of sawtooth and fishbones [15]. Therefore, it is difficult to discuss the onset condition of the seed magnetic islands observed in experiments from the point of view of the critical amplitude for the rapid growth of the magnetic island found in the previous research [5–7]. As shown in this study, it is possible to explain the rapid growth of magnetic islands and the onset of NTM after several pulses of a periodic MHD phenomenon such as sawtooth, fishbones, and ELM by taking into account the cumulative effect of the magnetic island width.

[1] R. Carrera, R.D. Hazeltine and M. Kotschenreuther, Phys. Fluids **29**, 899 (1986).
[2] A.M. Garofalo *et al.,* Phys. Rev. Lett. **89**, 235001 (2002).
[3] R.A. Moyer *et al.,* Phys. Plasmas **12**, 056119 (2005).
[4] F. Wagner *et al.*, Phys. Rev. Lett. **49**, 1408 (1982).
[5] R. Fitzpatrick, Phys. Plasmas **5**, 3325 (1998).
[6] R. Fitzpatrick, Phys. Plasmas **10**, 1782 (2003).
[7] Y. Ishii *et al.*, Nucl. Fusion **47**, 1024 (2007).
[8] S. von Goeler, W. Stodiel and N. Sauthoff Phys. Rev. Lett. **33**, 1201 (1974).
[9] H.R. Strauss *et al.*, Phys. Fluids **19**, 134 (1982).
[10] A. Hasegawa and L. Chen, Phys. Rev. Lett. **32**, 454 (1974).
[11] X. Wang *et al.*, Phys. Plasmas **5**, 2291 (1998).
[12] Y. Ishii and A. Smolyakov, Plasma Fusion Res. **3**, 048 (2008).
[13] O. Sauter *et al.*, Phys. Rev. Lett. **88**, 105001 (2002).
[14] R.J. Buttery *et al.*, Nucl. Fusion **44**, 69 (2003).
[15] M.F.F. Nave *et al.*, Nucl. Fusion. **43**, 179 (2003).
[16] R.J. Buttery *et al.*, Phys. Rev. Lett. **88**, 125005 (2002).
[17] R.C. Wolf *et al.*, Plasma Phys. Control Fusion **41**, B93 (1999).
[18] A. Gude *et al.*, Nucl. Fusion. **42**, 53 (2000).
[19] R.L. La Haye *et al.*, Nucl. Fusion. **40**, 53 (2000).
[20] O. Sauter *et al.*, Phys. Plasmas **4**, 1654 (1997).